

Supporting Information

Advancing Diagnostics with BODIPY-Bismuthene DNA Biosensors.

Laura Gutiérrez-Gálvez^a, Estefanía Enebral-Romero^{a,b}, Miguel Ángel Valle Amores^c, Clara Pina Coronado^a, Iñigo Torres^d, David López-Diego^e, Mónica Luna^e, Alberto Fraile^{c,f}, Félix Zamora^{d,g}, José Alemán^{c,f}, Jesús Álvarez^{g,h,i,j}, María José Capitán^{i,k}, Encarnación Lorenzo^{a,b,f} and Tania García-Mendiola^{a,f}.

^a Departamento de Química Analítica y Análisis Instrumental. Universidad Autónoma de Madrid. 28049, Madrid (Spain).

^b IMDEA-Nanociencia, Ciudad Universitaria de Cantoblanco. 28049, Madrid (Spain).

^c Departamento de Química Orgánica. Universidad Autónoma de Madrid. 28049, Madrid (Spain).

^d Departamento de Química Inorgánica. Universidad Autónoma de Madrid. 28049, Madrid (Spain).

^e Instituto de Micro y Nanotecnología IMN-CNM, CSIC (CEI UAM+CSIC), Isaac Newton 8. Tres Cantos. 28760, Madrid (Spain).

^f Institute for Advanced Research in Chemical Sciences (IAdChem). Universidad Autónoma de Madrid. 28049, Madrid (Spain).

^g Condensed Matter Physics Center (IFIMAC). Universidad Autónoma de Madrid. 28049, Madrid (Spain).

^h Departamento de Física de la Materia Condensada, Universidad Autónoma de Madrid, 29049-Madrid, (Spain).

ⁱ Física de sistemas crecidos con baja dimensionalidad, Universidad Autónoma de Madrid, Unidad Asociada al CSIC por el IEM, DP

^j Instituto de Ciencia de Materiales “Nicolás Cabrera”, Univ. Autónoma de Madrid, 28049-Madrid, (Spain).

^k Instituto de Estructura de la Materia IEM-CSIC, 28006-Madrid (Spain).

*Corresponding author: tania.garcia@uam.es

Results and discussion

Spectroscopic and microscopic characterization of FLBH

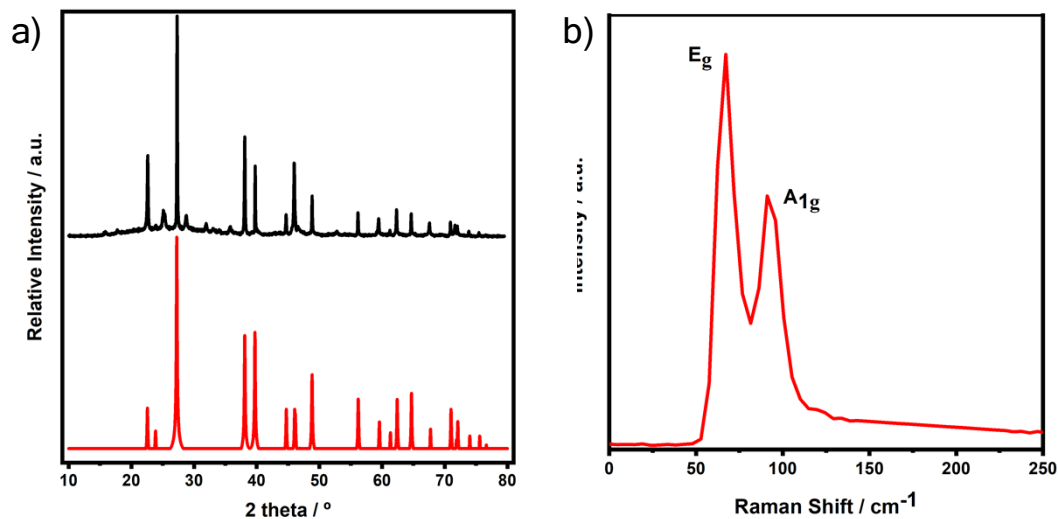


Figure S1. XRPD pattern (A) of the FLBH powder (black line) and the pattern corresponding to the simulated b-bismuth (red line). Raman spectra (B) of FLBH powder.

Figure S2. Topographic AFM image (**a**) of FLBHs on SiO₂. A large-scale AFM image of FLB hexagons used for the height statistical analysis in (**b**). Topographic AFM images (**c**) of some representative isolated FLBH on SiO₂ (down, their height profiles along the lines of the images in c).

The synthesized FLBHs have thicknesses ranging from 10 to 45 nm (Fig. S2b), with approximately 70% measuring between 15 and 30 nm. Considering the interlayer distance of bismuth is approximately 0.34 nm (3.38 Å), the estimated number of layers in the FLBHs ranges from roughly 44 to 88.

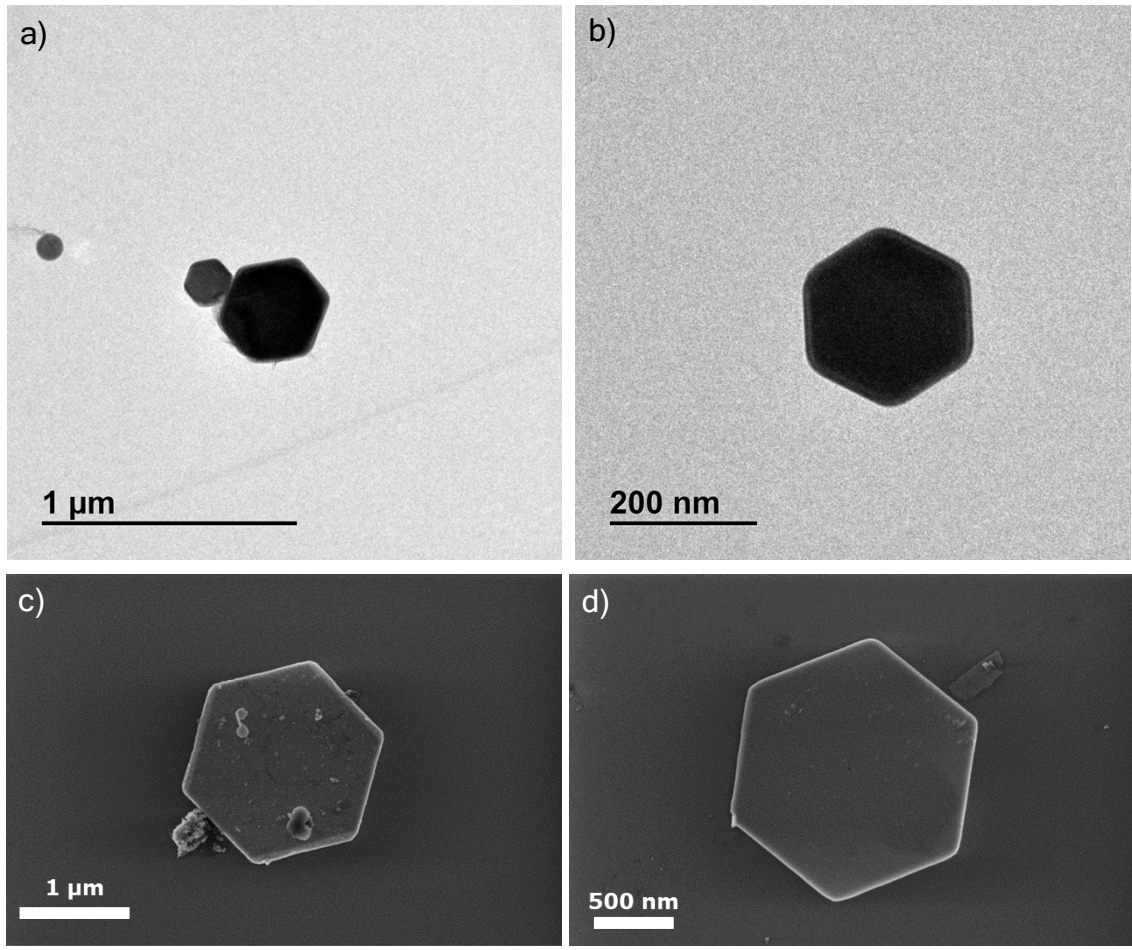


Figure S3. Transmission electron microscopy (**A, B**) and scanning electron microscopy (**C, D**) images of FLBHs.

Development of the biosensor for the detection of SARS-CoV-2

The results showed in Figure S4 reveal a more heterogeneous surface compared to the bare CSPE sample (Figure 1A and 1B of the main manuscript). In the backscattered electron images of CSPE/FLBH (Figure S4B), the brighter contrast regions indicate the presence of bismuthene nanoflakes, which have a higher atomic weight, while the darker areas correspond to the underlying CSPE, primarily composed of carbon. This is further supported by the EDX spectra, which not only show the characteristic carbon peak but also confirm the presence of Bi, verifying the successful incorporation of FLBH.

The number of FLBH flakes deposited on the CSPE surface have been estimated, considering that the thickness of a FLBH flake is between 15 and 30 nm. Figure S5 shows the AFM images and the study of the profile of different zones in a FLBH-modified CSPE (FLBH/CSPE). As can be observed in the images, the profile has been measured from an

area that was not covered by FLBH to a modified area. The average height value that can be estimated for the FLBH/CSPE platform is about 70 nm, so it could be stated that there are between 2 and 4 FLBH flakes on the electrode surface.

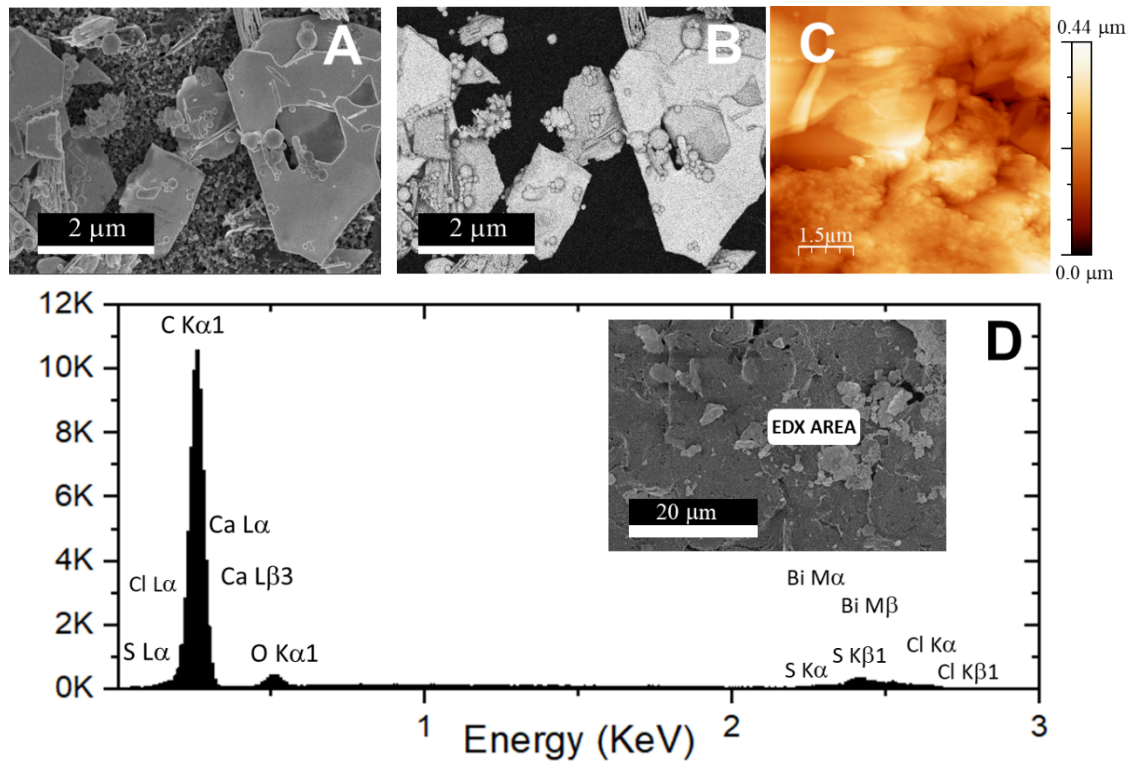


Figure S4. Secondary electron images, SEM (**A**), Backscattered electrons images, BSE (**B**), EDX (**D**) and AFM (**C**) characterization of FLBH/CSPE.

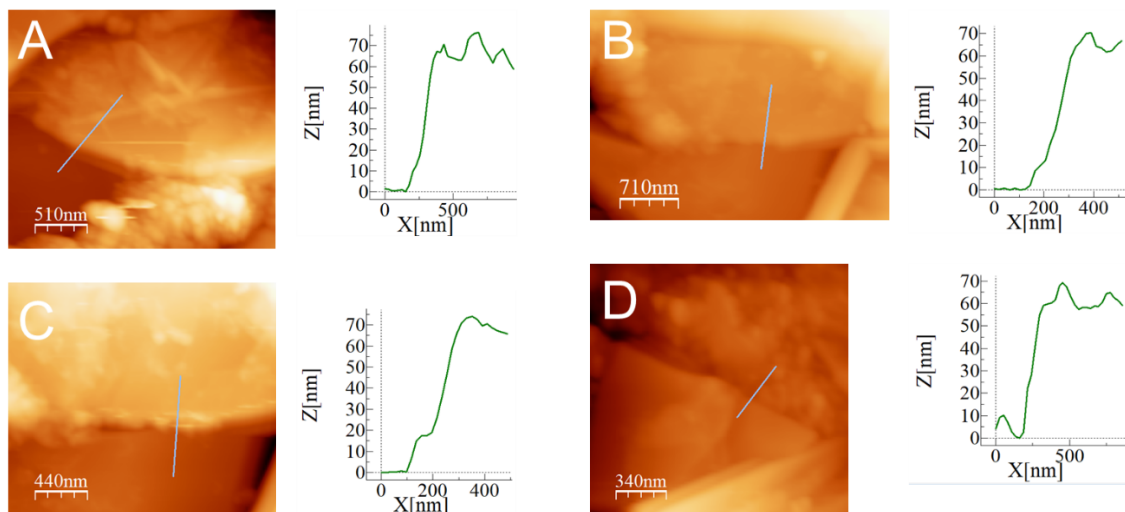


Figure S5. AFM topographic images and profile study of different areas of the FLBH/CSPE platform.

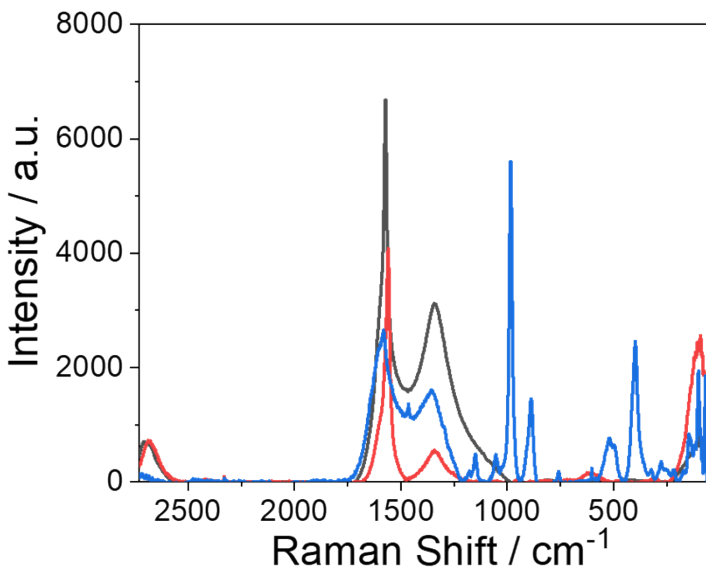


Figure S6. Raman spectra of a bare CSPE (black line), a CSPE modified with FLBH (FLBH/CSPE, red line) and a CSPE modified with FLBH and the probe sequence (Probe-SH/FLBH/CSPE, blue line).

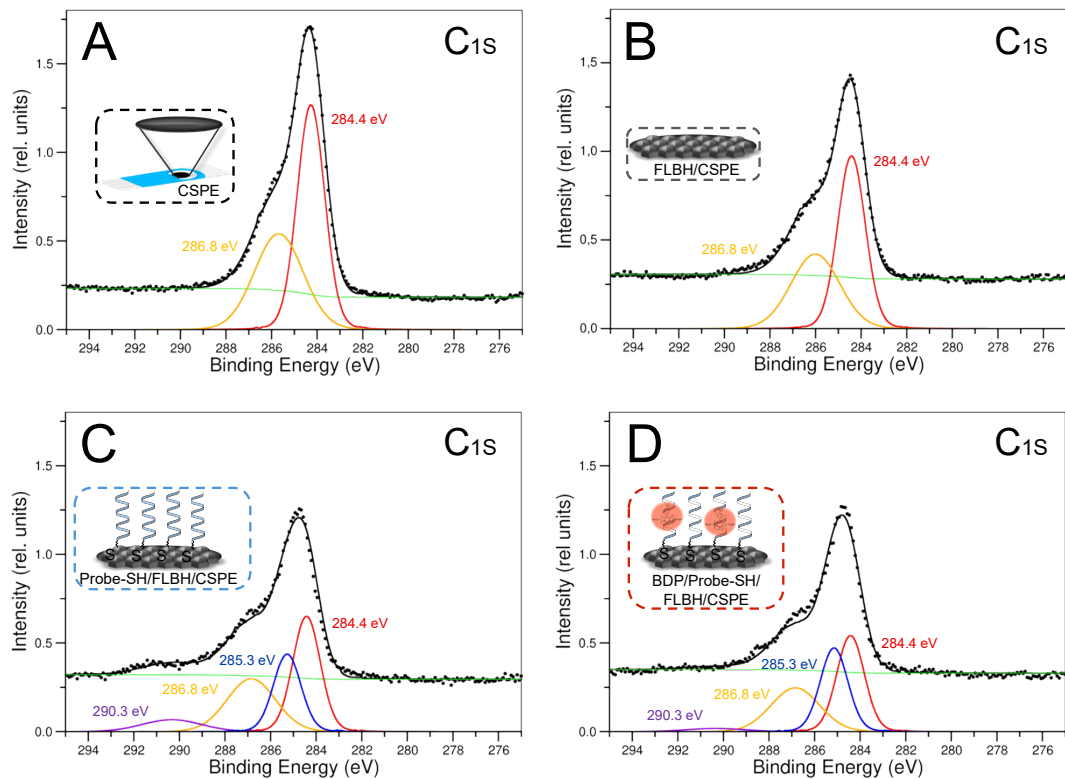


Figure S7. X-ray photoelectron spectroscopy (XPS) for the C1s of a bare CSPE (**A**), of the FLBH/CSPE platform (**B**), the Probe-SH/FLBH/CSPE one (**C**) and the BDP/Probe-SH/FLBSH/CSPE platform (**D**).

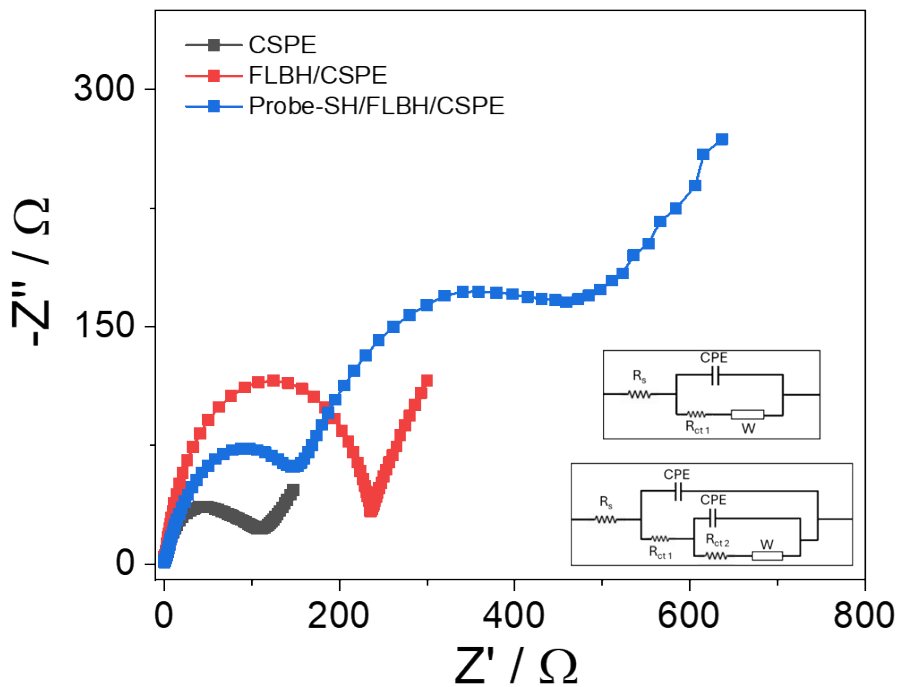


Figure S8. Nyquist plot of a bare CPE (black line), a the FLBH/CSPE platform (red line), and for the Probe-SH/FLBH/CSPE biosensing platform (blue line) in 10 mM $K_3Fe(CN)_6$ with 10 mM $K_4Fe(CN)_6$ in PB 0.1 M pH 7.0. EIS conditions: 0.12 V, 100 kHz to 0.01 Hz, and 10 mV amplitude.

SARS-CoV-2 virus detection

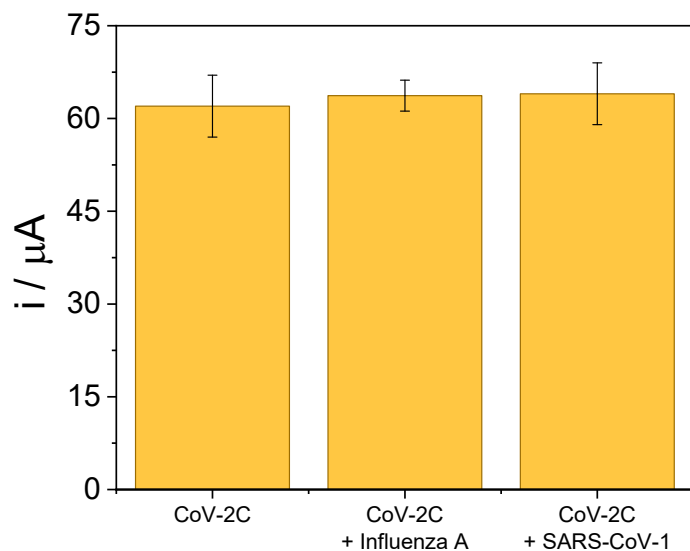


Figure S9. Bar diagram of the biosensor's response for 10.0 fM of the SARS-CoV-2 sequence (CoV-2C) in the absence and in the presence of other interfering viral sequences, Influenza A and SARS-CoV-1, at the same concentration.

Table S1. Comparative table of other biosensors reported in the literature for the specific SARS-CoV-2 virus detection.

Biosensor	Based on	Method	LOD	Reference
BODIPY-bismuthene DNA biosensor (SARS-CoV-2 sequence)	FLBH, BDP-NaSO ₃	DPV	4.97 fM	This work
Gold nanotriangles-electrochemical DNA biosensor (RdRp sequence)	AA, AuNTs/CSPE	DPV	36.3 fM	Del Caño et al. ¹
Electrochemical DNA biosensor (ORF1ab sequence)	MoS ₂ / CSPE	DPV	1.01 pM	Martínez-Periñán et al. ²
Electrochemical biosensor (SARS-CoV-2 RNA)	CHA and TdT-induced polymerization, Ru(NH ₃) ₆ ³⁺	DPV	26 fM	Peng et al. ³
Optical aptasensor (SARS-CoV-2 S protein)	POF/Au/PEG	Plasmonic/SPR	37 nM	Cennamo et al. ⁴

References

- R. del Caño, T. García-Mendiola, D. García-Nieto, R. Álvaro, M. Luna, H. A. Iniesta, R. Coloma, C. R. Diaz, P. Milán-Rois, M. Castellanos, M. Abreu, R. Cantón, J. C. Galán, T. Pineda, F. Pariente, R. Miranda, Á. Somoza and E. Lorenzo, *Microchim Acta*, 2022, **189**, 171.
- E. Martínez-Periñán, T. García-Mendiola, E. Enebral-Romero, R. del Caño, M. Vera-Hidalgo, M. Vázquez Sulleiro, C. Navío, F. Pariente, E. M. Pérez and E. Lorenzo, *Biosensors and Bioelectronics*, 2021, **189**, 113375.
- Y. Peng, Y. Pan, Z. Sun, J. Li, Y. Yi, J. Yang and G. Li, *Biosensors and Bioelectronics*, 2021, **186**, 113309.

4N. Cennamo, L. Pasquardini, F. Arcadio, L. Lunelli, L. Vanzetti, V. Carafa, L. Altucci
and L. Zeni, *Talanta*, 2021, **233**, 122532.